

Reduced Lantadenes A and B: semi-synthetic synthesis, selective cytotoxicity, apoptosis induction and inhibition of NO, TNF- α production in HL-60 cells

Suthar Sharad Kumar · Navin Tailor ·
Hong Boon Lee · Manu Sharma

Received: 17 August 2012 / Accepted: 8 November 2012 / Published online: 22 November 2012
© Springer Science+Business Media New York 2012

Abstract The aim of this study was to investigate the effect of pentacyclic triterpenoids-reduced Lantadenes A (**3**) and B (**4**) on the cytotoxicity, stimulation of apoptosis and regulation of transcription factors in HL-60 cells. The **3** and **4** are the minor compounds of weed *Lantana camara* L. (Verbenaceae) and were prepared semi-synthetically in single step by reducing Lantadenes A (**1**) and B (**2**) under microwave irradiation with yield of 98–99 %. The **3** and **4** demonstrated selective cytotoxicity against HL-60, MCF-7, HSC-2, and HCT-116 cancer cell lines (IC₅₀ 1.2–6.4 μ M) and were found non-toxic toward normal cells (VERO) with IC₅₀ >50). The compounds **3** and **4** (15 μ M)-induced apoptosis by activation of caspase-3 and bax, along with significant decrease in expression of NF- κ B (p-65) and bcl-2 in HL-60 cells. The compounds **3** and **4** at 15 μ M significantly suppressed the production of nitrite, TNF- α , and iNOS gene expression in HL-60 cells. The results suggested that reduced Lantadenes A and B have the potential to be developed as anticancer agents.

Keywords Reduced Lantadenes A and B · Cytotoxicity · Apoptosis · Transcription factors · NO · TNF- α

Electronic supplementary material The online version of this article (doi:10.1007/s00044-012-0354-x) contains supplementary material, which is available to authorized users.

S. S. Kumar · N. Tailor · M. Sharma (✉)
Department of Pharmacy, Jaypee University of Information
Technology, Distt. Solan, Wagnaghat 173234, Himachal
Pradesh, India
e-mail: lantadene@hotmail.com

H. B. Lee
Drug Discovery Laboratory, Cancer Research Initiative
Foundation, 12A Jalan TP5, Taman Perindustrian UEP, 47600,
Subang Jaya, Selangor Darul Ehsan, Malaysia

Introduction

Natural products are one of the major sources of lead molecules and pharmaceuticals. As far as plants are concerned, tropical forests are the most promising habitat for this search due to high biodiversity and endemism (Abelson, 1990). The role of weeds in the present pharmacopeia has been overlooked, despite significant evidence that weeds in particular, are an important source of medicines for indigenous peoples and have a highly significant over representation in indigenous pharmacopoeias in relation to other types of plants (Stepp and Moerman, 2001). There are numbers of evidences that weeds are relatively high in bioactive secondary compounds and are thus likely to hold promise for drug discovery. One such weed, which has attracted a lot of interest of scientists in last two decade, is *Lantana camara* L. (Verbenaceae). It has encroached upon vast expanse of land area including pastures, orchards, tea gardens forests and agricultural lands in tropical and subtropical parts of the world and has imposed a great threat to grazing livestock and overall ecological balance (Ghisalberti, 2000). However, it is a rich source of a number of biologically active triterpenoids. Lantadenes A (**1**), B (**2**), reduced Lantadenes A (**3**) and B (**4**) are such triterpenoids which have shown the potential to be developed as anticancer agents.

The pentacyclic triterpenoids **1** and **2** are the major constituents of the leaves of common pink-edged red flowering variety of weed *Lantana camara* L. (Verbenaceae). They constitute nearly 2.2 % of the dry weight of the leaf samples and are in the ratio 2:1, whereas, reduced Lantadene A (**3**) and Lantadene B (**4**) are minor constituents and are present to the extent of nearly 0.04 % (Sharma *et al.*, 1997). In last two decades extensive research was carried out on lantadenes/congeners and they have shown promising antitumor activity in various cancer models

(Inada *et al.*, 1995, 1997; Sharma *et al.*, 2007a, b, c; Sharma *et al.*, 2008, 2011; Kaur *et al.*, 2008, 2010). The triterpenoids **3** and **4** have shown antitumor activity against Epstein–Barr virus activation in Raji cells (Inada *et al.*, 1997), and the presence of hydroxyl group at C-3 position makes them good candidates for hybrid compound synthesis and structural modifications. As these compounds are present in minute amount in plant, no work has been done on their effect on cancer cytotoxicity and antitumor mechanism of these compounds. The purpose of present study was to first prepare **3** and **4** in sufficient quantity and then to evaluate cytotoxicity, apoptosis induction, and regulation of transcription factors by these compounds in HL-60 cells.

Results

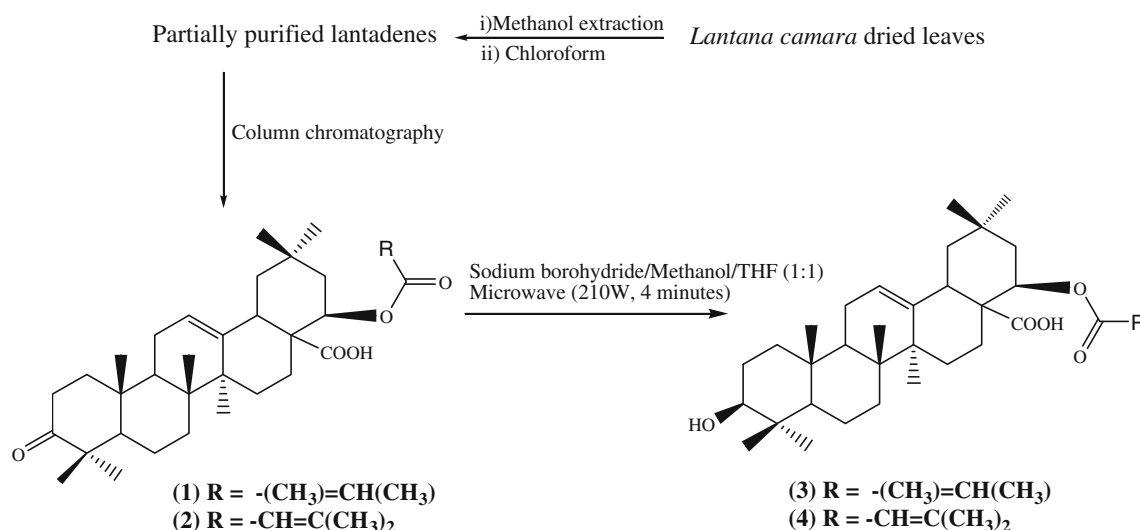
Preparation of reduced Lantadenes A and B

The reduced Lantadenes A and B are minor constituents of leaves of weed *Lantana camara* L. and are present only 0.04 % of the dry weight of the leaf samples. The chemistry of these triterpenoids revealed that there is little structural variation between them, therefore, **3** and **4** have very similar physicochemical properties (Sharma *et al.*, 2007c). Due to this, the isolation of **3** and **4** in sufficient quantity is very tedious and thus hampers the structural modifications/bioactivity of these compounds. To overcome isolation problem, the more abundant triterpenoids of lantana, i.e. Lantadenes A and B can be easily reduced to obtain **3** and **4** in sufficient quantity. The Lantadenes A and B are present nearly 2.2 % of the dry weight of the leaf sample and are in the ratio of 2:1 and can be easily

converted to **3** and **4** by reduction with sodium borohydride in the presence of methanol and tetrahydrofuran under microwave irradiation (Scheme 1). The reduction with sodium borohydride generally requires a polar protic solvent, but Lantadenes A and B being non polar in nature were only sparingly soluble in methanol. Therefore, reduction was carried out in methanol and tetrahydrofuran (1:1) mixture. The reduction under microwave irradiation was completed in 4 min with yield of 98–99 %. This process selectively converted 3-oxo group into C-3 hydroxyl group of **3** and **4**. The structures were confirmed by combined use of spectroscopy and elemental analyses. The purity of compounds was assessed by HPLC and found to be more than 98 %.

Cytotoxicity studies

The MTT microassay was used for the evaluation of cytotoxic properties of the **1**, **2**, **3**, and **4**. The growth-inhibitory effects were undertaken in four human cell lines, including HL-60, HCT-116, HSC-2, and MCF-7. The compound **3** showed marked cytotoxicity with IC_{50} in the range of 1.2–6.1 μ M, whereas **4** showed cytotoxicity with IC_{50} in the range of 1.8–6.4 μ M. The compounds were found to be most potent against HL-60 followed by HCT-116, HSC-2, and MCF-7 cell lines (Table 1). These compounds showed selective toxicity toward cancer cells and were not found toxic toward normal cells (VERO). The compounds **3** and **4** were found to be more cytotoxic than parent compounds **1** and **2** and results indicated that C-3-OH group is critical for the cytotoxicity and C-3 keto group led to decrease in the cytotoxicity. The compound **3**, having angeloyloxy side chain was found more potent than compound **4**.



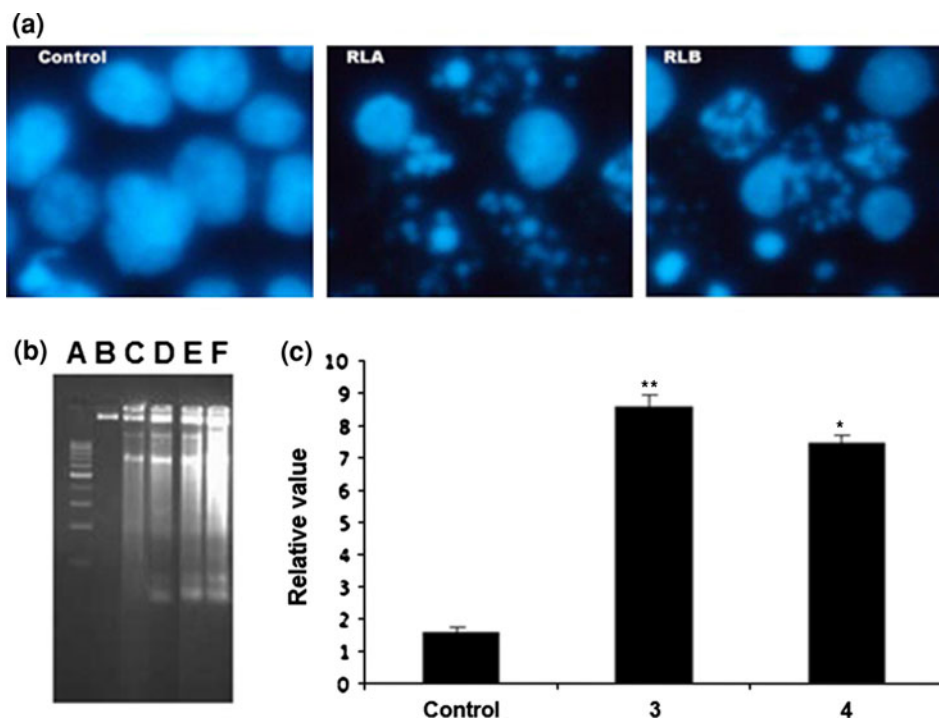
Scheme 1 Sequence of steps involved in isolation of Lantadenes A (**1**) and B (**2**) and preparation of reduced Lantadenes A (**3**) and B (**4**)

Table 1 In vitro cytotoxicity studies of **1**, **2**, **3**, and **4** against cancer cell lines after 48 h IC₅₀ ±SD (μM)

Compounds	HCT-116	HSC-2	MCF-7	HL-60	VERO
1	13.4 ± 1.9	50.7 ± 1.2	25.8 ± 6.4	19.3 ± 1.8	>50
2	13.2 ± 2.5	43.0 ± 13.6	81.4 ± 1.9	19.1 ± 3.3	>50
3	1.2 ± 0.2	6.1 ± 2.1	6.0 ± 1.7	1.5 ± 0.5	>50
4	1.8 ± 0.5	6.4 ± 1.2	5.2 ± 1.4	2.1 ± 0.8	>50
Cisplatin	17.5 ± 1.2	21.3 ± 9.1	18.4 ± 1.4	2.4 ± 0.0	0.03 ± 0.00

Results are given as mean of three independent experiments with triplicates in each experiment

Fig. 1 a Apoptosis observed by Hoechst 33258 staining. Marked morphological changes such as apoptotic bodies, nuclear fragmentation were seen at 15 μM treatment of **3** and **4**, respectively, after 24 h; **b** Dose-dependent induction of DNA fragmentation by **3** and **4** in HL-60 cells. A DNA marker, B control cells, C cells treated with 10 μM of **3**, D cells treated with 15 μM of **3**, E cells treated with 10 μM of **4**, F cells treated with 15 μM of **4**; **c** Caspase-3 activation by **3** and **4** at 15 μM after 24 h



Apoptosis induction and DNA fragmentation

To determine the morphological effects, **3** and **4**-treated HL-60 cancer cells were observed under a fluorescence microscope. Uniform normal morphology was seen in the control group, whereas, fragmented chromatin and apoptotic bodies were seen in the cells treated with **3** and **4** (Fig. 1a). In addition, a typical DNA strand-break was observed by means of gel electrophoresis. The HL-60 cancer cells were incubated in the presence of **3** and **4** at various concentrations for 24 h and DNA was isolated from HL-60 cells. The characteristic ‘ladder’ pattern of apoptosis was observed at 15 μM of **3** and **4** (Fig. 1b).

Flow cytometric analysis

To assess whether compounds **3** and **4**-induced growth inhibition of the cells is mediated via alterations in cell cycle regulation and apoptosis, the effect of compounds **3**

and **4** on cell cycle distribution was evaluated. When the HL-60 cells were treated with 15 μM of compounds **3** and **4**, the percentage of cells in the G₁-phase was substantially lower as compared to control at all treatment periods. The decrease in the G₁-phase was reflected in a slight increased S-phase population after 3–9 h of treatment and an apparently increased G₂/M-phase population after 6–12 h was observed in comparison to control. The results indicated that **3** and **4** suppress cell proliferation by causing cell cycle arrest in the G₂/M phase (Table 2).

Caspase-3-dependent induction of apoptosis

We next examined the effects of reduced Lantadenes A and B on the activation of caspase-3, an active executor of apoptosis. Both compounds **3** and **4** (15 μM)-induced the activation of caspase-3 in HL-60 cells after 24 h of incubation (Fig. 1c). The compound **3** was found to be more potent in terms of activation of caspase-3, in comparison to compound **4**.

Table 2 Effect of **3** and **4** (15 μ M) on HL-60 cell cycle distribution by flow cytometric analysis

Compounds		Control	3 h	6 h	9 h	12 h
3	Sub-G1	0.1 \pm 0.0	0.2 \pm 0.1	0.4 \pm 0.2	1.2 \pm 0.4	3.2 \pm 1.2**
3	G0/G1	36.2 \pm 2.4	34.4 \pm 1.4	20.8 \pm 0.4***	14.0 \pm 0.6***	15.4 \pm 0.8***
3	S	56.8 \pm 2.4	57.0 \pm 0.7	64.2 \pm 0.8***	63.6 \pm 2.6***	44.8 \pm 0.8***
3	G2/M	9.0 \pm 1.2	8.4 \pm 0.8	15.8 \pm 0.8***	20.8 \pm 2.4***	42.0 \pm 0.8***
4	Sub-G1	0.1 \pm 0.0	0.3 \pm 0.1	0.5 \pm 0.2	1.4 \pm 0.2	3.4 \pm 1.2**
4	G0/G1	34.4 \pm 4.2	32.8 \pm 1.2	18.2 \pm 0.8***	12.6 \pm 0.6***	13.9 \pm 0.6***
4	S	54.2 \pm 1.4	55.1 \pm 0.6	62.1 \pm 0.4***	61.6 \pm 2.6***	42.1 \pm 0.6***
4	G2/M	8.2 \pm 0.4	7.4 \pm 0.6	14.8 \pm 0.8***	19.9 \pm 0.9***	40.8 \pm 1.8***

The data is presented as mean \pm SD from three independent experiments. ** $p < 0.01$; *** $p < 0.001$; compared with control

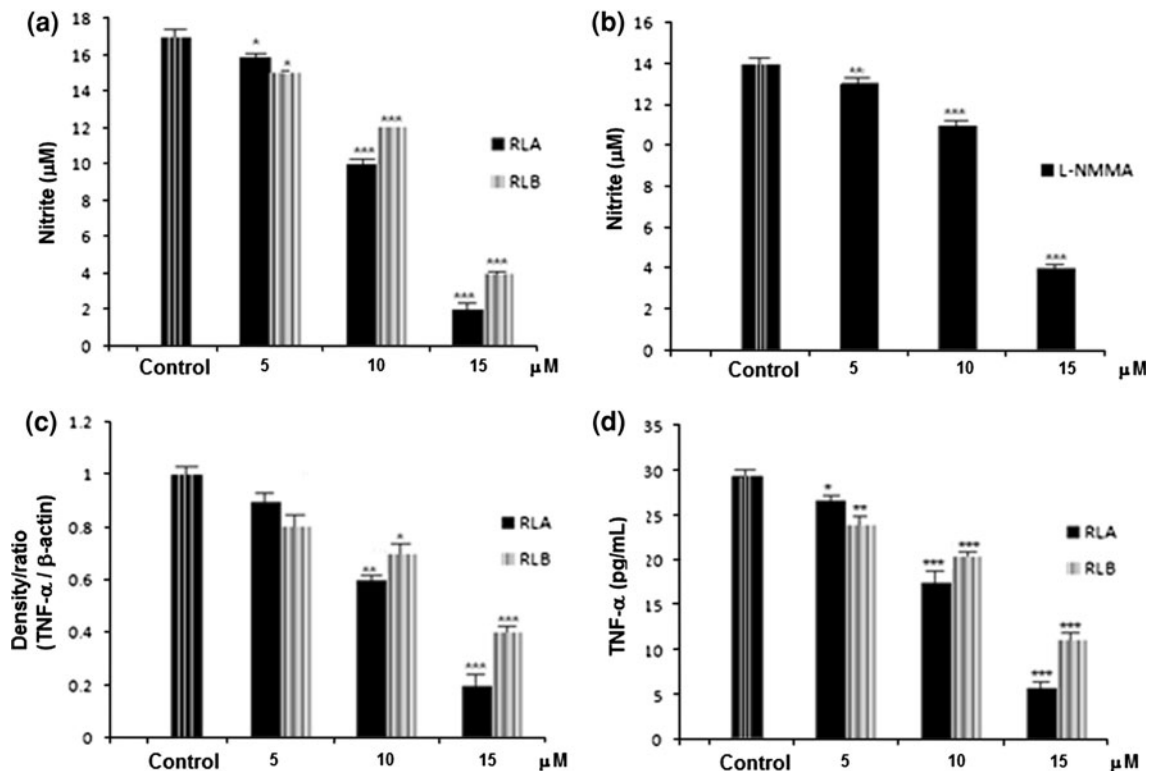


Fig. 2 **a** Effects of **3** and **4** on nitrite production; **b** Effects of L-NMMA on nitrite production in HL-60 cells; **c** Effects of **3** and **4** on the levels of TNF- α mRNA; **d** Effects of **3** and **4** on TNF- α

production. Values are the means from four samples with the SEM shown by vertical bars. Statistical significance: * $p < 0.05$, ** $p < 0.01$, and *** $p < 0.001$ versus control

Inhibition of nitrite and TNF- α release and iNOS expression by compounds **3** and **4** in HL-60 cells

The release of nitrite was determined in HL-60 cells with/without treatment of compounds **3** and **4**. The results showed that **3** and **4** strongly inhibited the release of nitrite in HL-60 cells after 12 h in a concentration-dependent manner at 5–15 μ M (Fig. 2a). The L-NMMA, a non-specific inhibitor of iNOS, also suppressed nitrite production in HL-60 cells at 5–15 μ M (Fig. 2b). The normal unstimulated HL-60 cells released TNF- α (28.7 pg/ml) into the medium after 6 h of incubation. The treatment with compounds **3** and **4** dose-dependently inhibited TNF- α

release (Fig. 2c, d) from HL-60 cell. The iNOS expression was also suppressed by compounds **3** and **4** in a concentration-dependent manner (Fig. 3). These findings indicated that compounds **3** and **4** inhibit the release of nitrite and TNF- α through the inhibition of iNOS expression. The compound **3** showed better inhibition of NO, TNF- α , and iNOS gene expression than compound **4** in HL-60 cells.

Effect of compounds **3** and **4** on the mRNA expression for iNOS, bcl-2, bax, NF- κ B, and caspase-3

The iNOS, bcl-2, bax, NF- κ B, and caspase-3 genes were amplified against β -actin housekeeping gene. It was

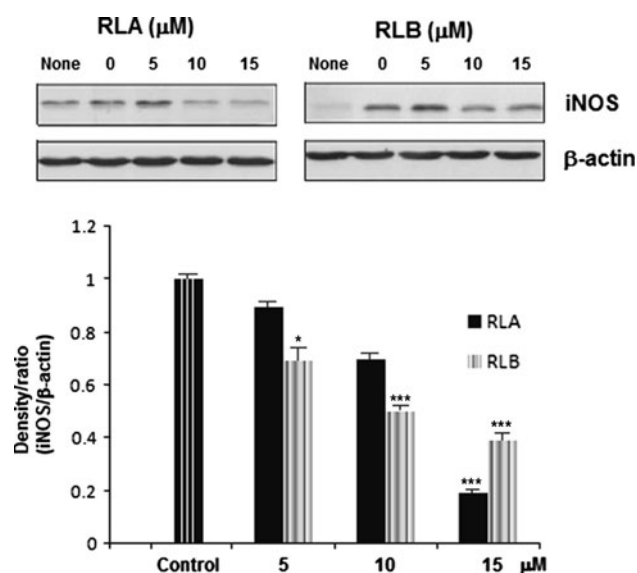


Fig. 3 Effects of **3** and **4** on iNOS expression and protein quantification by scanning densitometry

observed that treatment with compounds **3** and **4** (15 μM) down-regulated the expression of iNOS gene in comparison to control cells, which showed high expression of iNOS (Fig. 4). The treatment of HL-60 cells with compounds **3** and **4** (15 μM) down-regulated the expression of bcl-2 and NF- κB , whereas, the expression of bax and caspase-3 were up-regulated in HL-60 cells. The effect of compounds **3** and **4** on expression of bcl-2, bax, NF- κB , and caspase-3 gene is shown in Fig. 4.

Discussion

Triterpenoids play a very important role in a plant's defence mechanism and protect the plants from both constitutive and induced defensive responses against insects and environmental stress (Yadav *et al.*, 2010). Hence, triterpenoids provide a very good protection shield for plants, indicating their potential for use in the prevention of various cancers and inflammatory diseases in humans; however, mechanism of action is not fully understood. This investigation is about the anticancer effect of pentacyclic triterpenoids-reduced Lantadenes A and B. The reduced Lantadenes A and B have shown potential and selective toxicity toward cancer cells and were found to be more cytotoxic than parent compounds **1** and **2** and standard drug cisplatin. The results of cytotoxicity studies indicated that conversion of C-3 keto group to C-3-OH increased the activity, and C-22 angeloyloxy side chain was found to be critical for the cytotoxicity. The compounds **3** and **4** showed cell cycle arrest in the G₂/M phase and marked

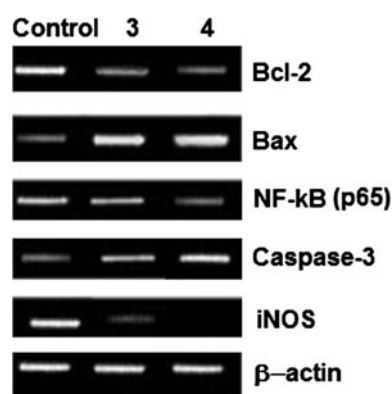


Fig. 4 Expression of transcription factors detected by RT-PCR before and after cells was treated with 15 μM of **3** and **4**

morphological changes like fragmented chromatin and apoptotic bodies formation in HL-60 cells. The induction of cell cycle arrest is a common mechanism proposed for the cytotoxic effects of many anticancer-drugs along with apoptosis. The cell cycle arrest can trigger proliferation inhibition and apoptosis in cancer cells (Chao *et al.*, 2004). Cell cycle checkpoints are important control mechanisms that ensure the proper execution of cell cycle events. During cell cycle, the G₂/M checkpoint is a potential target for cancer therapy. It prevents DNA-damaged cells from entering mitosis and allows for the repair of DNA damage (Taylor and Stark, 2001) and plays an important role in providing time for DNA repair, whereas apoptosis may function to remove irreparably damaged cells. The p53 can regulate the G₂/M transition either through the induction of p21 and 14-3-3 σ , a protein that normally sequesters cyclin B1–Cdc2 complexes in the cytoplasm (Hermeking *et al.*, 1997; Bunz *et al.*, 1998) or through the induction of apoptosis (Yonish-Rouach *et al.*, 1991). It is well-documented fact that the tumor antigen p53 is overproduced in transformed cells of various species, including man. HL-60 is an exceptional human tumor cell line that does not express this protein. Therefore, the G₂/M cell cycle arrest by compounds **3** and **4** was independent of p53. A number of marketed drugs like taxol, doxorubicin, and colchicines lead to G₂/M cell cycle arrest by down-regulation of Bcl-2 and increased Bax protein levels. Bcl-2 is known to play an important role in the intrinsic apoptosis pathway and protects the microtubule integrity (Haldar *et al.*, 1997). At the same time, bcl-2 family is crucial in determining cell fate in the apoptotic pathway and they influence mitochondrial membrane polarization and the cleavage-mediated caspase activation, which are the ultimate effectors in apoptosis signalling. Although, little is known about the transcriptional factors that control the expression of bcl-2-related proteins, yet NF- κB is the most important transcriptional factor involved in their regulation

(Crawford *et al.*, 2001). The diminished expression of bcl-2 and over-expression of pro-apoptotic protein bax has been observed in cells undergoing apoptosis. Both these compounds (**3**, **4**)-induced the apoptosis by down-regulating bcl-2, NF- κ B expression and activating bax expression in HL-60 cells.

It is known that caspases are specific proteases of apoptosis, particularly caspase-3 and the activated caspase-3 has been shown to cleave-specific substrates including the nuclear protein PARP, involved in DNA repair and genomic maintenance (Lopez-Beltran *et al.*, 2007). The compounds **3** and **4** were found to trigger apoptosis by activating caspase-3 mRNA expression in HL-60 cells. In last one decade role of NO and iNOS have been extensively studied in cancer cells and it has been over expressed in number of tumors (Sethi *et al.*, 2012). The role of NO in tumor development is ambiguous. When produced by tumor cells, NO may induce vasodilation resulting in enhanced permeability in tumor vasculature. In such cases, blood flow in the tumor will be increased, which would provide favorable condition for tumor growth (Gallo *et al.*, 1998). In this study, the compounds **3** and **4** were found to inhibit nitrate levels as well as down-regulate iNOS mRNA expression in HL-60 cells. Tumor necrosis factor- α is the central mediator of tumor promotion and overproduction of TNF- α by tumor cell lines has been shown to stimulate growth of human cancer cell and metastasis of sarcoma cells (Manchester *et al.*, 1993). The compounds **3** and **4** also suppressed TNF- α production in HL-60 cells. The binding of TNF- α with its cell surface receptors has been shown to activate complex signal transduction pathways, including activation of NF- κ B, and induction or down-regulation of growth regulatory genes such as bcl-2 (Hong *et al.*, 2000). Therefore, suppression of TNF- α production may be related to down regulation of NF- κ B and bcl-2 in HL-60 cells by the compounds **3** and **4**.

Conclusion

The apoptosis induction by reduced Lantadenes A and B represent one of the possible mechanisms that could account for their antineoplastic activities. Activation of caspase-3 as well as bax and down-regulation of NF- κ B and bcl-2 might play an important role in reduced Lantadenes A and B-induced apoptosis in HL-60 cells. The reduced Lantadenes A and B also regulated NO, iNOS gene expression and TNF- α production in HL-60 cells, which may further be related to the down regulation of NF- κ B and bcl-2. The data presented here contribute further to understand the possible mechanisms of anticancer activity of reduced Lantadenes A and B.

Materials and methods

The reaction was monitored and purity of all compounds was established by single spot on the Merck precoated silica gel TLC plates and iodine vapors were used for the detection. Melting points were determined on an Indosati digital melting point apparatus and were uncorrected. IR spectra were recorded on a Perkin Elmer-spectrum RX-IFTIR, using potassium bromide pellets. ^1H NMR and ^{13}C NMR spectra were recorded with Bruker AVANCE II 400 MHz spectrometer using CDCl_3 as solvent, and tetramethylsilane was used as internal standard. Mass spectra were obtained with Micromass 70-VSE mass spectrometer at 70 eV using electronionization (EI). Elemental analysis of compounds was within $\pm 0.04\%$ of the theoretical values. All solvents were freshly distilled and dried prior to use according to standard procedures.

Plant material

Leaves of *Lantana camara* were collected in September 2011 from Palampur (HP), India. The sample was identified by Dr. Sunil Dutta, Research Officer, National Medicinal Plant Board, New Delhi. The leaves were shade-dried and powdered and the voucher specimen (LC; 097 JUIT) was deposited in the Herbarium at the Jaypee University of Information Technology Warknaghat, India.

Lantadenes A and B isolation

Lantadenes A and B were isolated in pure form as described in previous reports and the purity of Lantadenes A and B were confirmed by spectral and elemental analysis and found to be same as that of earlier reports (Sharma *et al.*, 1987; Sharma and Sharma, 2006).

Microwave-assisted reduction of Lantadenes A and B

The sequence of steps involved in conversion of Lantadenes A and B to reduced Lantadenes A and B is shown in Scheme 1. To 100 mg (0.18 mM) of **1** and **2** and 6.80 mg (0.18 mM) of sodium borohydride were separately subjected for microwaves irradiations at 210 W (30 %) for 1–4 min in a 2 ml solution of methanol (1 ml) and tetrahydrofuran (1 ml). The reaction was monitored on TLC after every 1 min and was incomplete up to 3 min and at 4 min reaction was completed to afford **3** and **4**, respectively. After completion of reactions dilute HCl solution was added to quench the unused NaBH_4 . The organic solvents were evaporated in rota evaporator and precipitated reduced Lantadenes were extracted with dichloromethane (DCM). The solvent was removed under reduced pressure to give **3** (TLC, petroleum ether: ethyl acetate; 4:1, R_f 0.31) and **4**,

(TLC, petroleum ether: ethyl acetate; 4:1, R_f 0.28). The product was recrystallized from methanol.

22β-[(3-Methyl-1-oxo-2-butenyl) oxy]-3β-hydroxyolean-12-en-28-oic acid (3)

White crystals (yield 100.6 mg, 99.70 % w/w), m.p. 278–279 °C, IR (ν_{\max} , KBr, cm^{-1}): 3482.87 (3-OH stretch), 2948.99, 2827.53 (C–H stretching), 1717.87 (ester, C=O), 1701.25 (acid, C=O), ^1H NMR (DMSO- d_6 , δ ppm), 6.00 (1H, *m*, C-3'-H), 5.31 (1H, *t*, C-12-H), 4.99 (1H, *t*, C-22-H), 3.09 (1H, *t*, $J = 7.82$, C-3-H), 3.00 (1H, *d*, C-18-H), 1.16 (3H, *s*, CH_3), 1.09 (3H, *s*, CH_3), 1.06 (3H, *s*, CH_3), 0.99 (3H, *s*, CH_3), 0.85 (3H, *s*, CH_3), 0.83 (3H, *s*, CH_3). ^{13}C NMR (CDCl_3 , δ ppm): 38.77 (C-1), 36.51 (C-2), 79.28 (C-3), 45.71 (C-4), 54.77 (C-5), 20.11 (C-6), 32.30 (C-7), 40.25 (C-8), 47.06 (C-9), 38.09 (C-10), 23.74 (C-11), 121.53 (C-12), 158.43 (C-13), 41.46 (C-14), 27.90 (C-15), 25.40 (C-16), 49.59 (C-17), 38.99 (C-18), 43.96 (C-19), 29.59 (C-20), 38.29 (C-21), 75.60 (C-22), 26.96 (C-23), 15.57 (C-24), 15.18 (C-25), 16.49 (C-26), 26.68 (C-27), 177.14 (C-28), 33.43 (C-29), 25.77 (C-30), 165.70 (C-1'), 127.50 (C-2'), 137.42 (C-3'), 15.00 (C-4'), 22.89 (C-5'). ESI-MS (m/z): 555.5 [$M + 1$], *anal.* $\text{C}_{35}\text{H}_{54}\text{O}_5$, C, 75.77 %, H, 9.81 %, found C, 75.75 %, H, 9.80 %.

22β-[(3-Methyl-1-oxo-2-butenyl) oxy]-3β-hydroxyolean-12-en-28-oic acid (4)

White crystals (yield 99.26 mg, 98.90 % w/w), m.p. 276–278 °C, IR (ν_{\max} , KBr, cm^{-1}): 3480.79 (3-OH stretch), 2949.59, 2875.08 (C–H stretching), 1717.98 (ester, C=O), 1701.98 (acid, C=O), ^1H NMR (CDCl_3 , δ ppm): 5.51 (1H, *d*, $J = 2.76$, C-2'-H), 5.31 (1H, *t*, C-12-H), 4.98 (1H, *t*, C-22-H), 3.15 (1H, *q*, $J = 4.56$, C-3-H), 2.95 (1H, *d*, C-18-H), 1.13 (3H, *s*, CH_3), 1.10 (3H, *s*, CH_3), 1.06 (3H, *s*, CH_3), 1.00 (3H, *s*, CH_3), 0.88 (3H, *s*, CH_3), 0.85 (3H, *s*, CH_3). ^{13}C NMR (CDCl_3 , δ ppm): 38.49 (C-1), 33.81 (C-2), 79.02 (C-3), 47.64 (C-4), 55.20 (C-5), 20.24 (C-6), 30.08 (C-7), 39.25 (C-8), 48.55 (C-9), 35.37 (C-10), 23.85 (C-11), 122.68 (C-12), 143.09 (C-13), 41.95 (C-14), 28.11 (C-15), 24.17 (C-16), 50.55 (C-17), 38.76 (C-18), 46.05 (C-19), 29.71 (C-20), 37.05 (C-21), 75.24 (C-22), 27.63 (C-23), 15.58 (C-24), 15.45 (C-25), 16.95 (C-26), 26.30 (C-27), 177.58 (C-28), 31.15 (C-29), 25.87 (C-30), 165.42 (C-1'), 116.05 (C-2'), 157.16 (C-3'), 23.51 (C-4'), 27.45 (C-5'). ESI-MS (m/z): 555.4 [$M + 1$], *anal.* $\text{C}_{35}\text{H}_{54}\text{O}_5$, C, 75.77 %, H, 9.81 %, found C, 75.72 %, H, 9.82 %.

Cancer cell culture and MTT assay

Human leukemic cells HL-60, colorectal carcinoma cells HCT116 and breast adenocarcinoma cells MCF7 were

purchased from the American Type Culture Collection (ATCC, USA). Human oral squamous carcinoma cells HSC-2 was obtained from the Health Science Research Resources Bank (Japan Health Sciences Foundation, Japan) and VERO was obtained from National Center for Cell Science, Pune. The HL-60, HCT116, MCF7, and VERO cells (African green monkey kidney fibroblast) were grown in RPMI medium supplemented with 10 % fetal bovine serum and 1 % penicillin–streptomycin (Gibco, Invitrogen, USA). For assay, phenol red-free RPMI medium (Sigma-Aldrich, USA) supplemented with 5 % fetal bovine serum and 1 % penicillin–streptomycin was used. For HSC-2, cells were maintained using MEM medium (Gibco, Invitrogen, USA) supplemented with 10 % fetal bovine serum and 1 % penicillin–streptomycin. The same complete growth medium was used for HSC-2 during assay. HL-60 (15,000 cells/well), HCT116 and MCF7 (3000 cells/well), and HSC-2 (4,000 cells/well) were seeded into 96-well plates and incubated overnight for cell attachment. For treatment, compounds were added at concentrations ranging from 0.01 to 100 μM and incubated for 48 h. At the end of incubation, 20 μl /well of 5 mg/ml thiazoyl blue tetrazolium bromide (MTT) (Amresco, USA) was added and cells were further incubated for 4 h. Supernatant was then removed and the purple formazan which has formed was dissolved using 100 μl of DMSO (Fisher Scientific, UK). Absorbance was read at 570 nm using Spectra Max M4 microplate reader (Molecular Devices Inc., US).

Morphological analysis by nuclear staining with Hoechst 33342

The nuclear morphology of cells was studied using the cell-permeable DNA dye Hoechst 33342. Cells with homogeneously stained nuclei were considered viable, whereas the presence of chromatin condensation and/or fragmentation was indicative of apoptosis (Gschwind and Huber, 1995). HL-60 cells were placed in 24-well plates at a concentration of 4×10^5 cells/ml. The cells were then treated with various concentrations of **3** and **4** and incubated for an additional 24 h. Then, Hoechst 33342, a DNA-specific fluorescent dye, was added to the culture medium at a final concentration of 10 $\mu\text{g}/\text{ml}$ and the plates were incubated for an additional 10 min at 37 °C. The stained cells were then observed under a fluorescence microscope equipped with a Cool SNAP-Pro color digital camera in order to determine the degree of nuclear condensation.

DNA fragmentation analysis

HL-60 cells were incubated with 0, 10, and 15 μM of **3** and **4** for 24 h at 37 °C. DNA fragmentation was analyzed by

electrophoresis as described earlier (Smith *et al.*, 1989). In brief, after exposure to trypsin, the cells (10^7 cells per sample) were washed with Tris-buffered saline (TBS) buffer (pH 7.6) and collected by centrifugation at $1,000\times g$ for 10 min. The pellet was re-suspended for 2 h at $50\text{ }^\circ\text{C}$ in a lysing solution made up of 10 mM Tris-HCl (500 μl , pH 8.0), 150 mM NaCl, 10 mM ethylenediamine tetraacetic acid (EDTA, edetic acid), 0.4 % sodium dodecyl sulfate (SDS), and 100 $\mu\text{g/ml}$ proteinase K. The lysate was then extracted with equal volumes of phenol/ CHCl_3 /isoamyl alcohol (25:24:01). The DNA was precipitated with ethanol (EtOH), air-dried and dissolved in TE buffer [5 mM Tris-HCl (pH 8.0) and 20 mM edetic acid-containing RNase A (0.1 mg/ml, Sigma)]. The samples were run in agarose gel-containing ethidium bromide (0.5 $\mu\text{g/ml}$) and were visualized under ultraviolet (UV) light.

Flow cytometric analysis

Cell cycle analysis by flow cytometry was performed, as described in a previous report (Sharma *et al.*, 2007a, b, c). After treatment, the cells were collected, washed with cold phosphate-buffered saline (PBS), and fixed with 70 % ice-cold ethanol at $-20\text{ }^\circ\text{C}$ overnight. Then, the cells were centrifuged and suspended in a staining solution containing 1 % Triton-X 100, 0.1 mg/ml RNase and 4 $\mu\text{g/ml}$ propidium iodide (PI) for 30 min at $37\text{ }^\circ\text{C}$ in the dark and analyzed by fluorescence-activated cell sorter flow cytometry (FACS-caliber, Becton-Dickinson, San Jose, CA, USA), using Cell Quest software. The data was finally analyzed with the Modfit 3.0 DNA software [23]. The proliferation index was calculated according to formula: Proliferation index = $(S + G2/G) \times 100 / G1 + S + G2 / M$, where S = DNA synthesis phase, G1 = Gap 1 phase, G2 = Gap 2 phase, M = mitosis phase.

Caspase-3 activity

Cells (1.5×10^6 cells/ml) were treated with the compounds **3** and **4** (at 15 μM) in 12-well plates for 24 h. Caspase-3 activity was measured using a Caspase-3 colorimetric assay kit (BioVision, USA). In brief, compounds **3** and **4**-treated cells were washed with PBS, and were lysed with cell lysis buffer for 1 min on ice. Each cell lysate was centrifuged at $10,000\times g$ for 1 min, and the supernatant was collected. After protein quantification using a DC protein assay kit (Bio-Rad Laboratories, USA), 50 μg protein was diluted to 50 μl with cell lysis buffer and to that, 50 μl reaction buffer was added. The absorbance of each sample mixture was measured at 400 nm. Finally, 5 μl 4 mM DEVD-pNA (caspase-3 substrate) was added to the mixture and incubated at $37\text{ }^\circ\text{C}$ for 1 h. The absorbance of the final reaction mixture was measured at the same wavelength.

RT-PCR analysis for iNOS, TNF- α , bcl-2, bax, NF κ B, and caspase-3

Logarithmically growing HL-60 cells (5×10^4) were incubated for 4 h in the presence and the absence of compounds **3** and **4** at a concentration of 15 μM . The cDNA was synthesized using Cells-to-DNA kit (Ambion Inc.). Cells from tissue culture were washed with PBS and heated in cell lysis II buffer (provided in the kit) to release the RNA into the solution. This is followed by a heating step to inactivate endogenous RNases. The genomic DNA is further degraded by treating with DNase followed by inactivation of DNase by heating at $70\text{ }^\circ\text{C}$. Reverse transcription was performed at $42\text{ }^\circ\text{C}$ for 50 min using Moloney murine leukaemia virus RT (supplied along with the kit). Gene expression studies were performed by PCR analysis. The mouse iNOS sense 5'CT TCAACACCAAGGTTGTCTGCAT-3' and antisense 3'AT GTCATGAGCAAAGGCCGAGAAC-5', TNF- α sense 5'-T TGACCTCAGCG CTGAGTTG-3' and antisense 5'-CCTG TAGCCCACGTCGTAGC-3', bcl-2 sense 5'-AGCTGCAC CTGACGCCCTT-3' and antisense 3'CCCAGCCTCCGTT ATTCTGGA-5', Bax (258 bp) sense 5'-ACCAAGAAGCT GAGCGAGTGTC-3' antisense 5'-TGTCCAGCCCATGA TGGTTC-3' NF- κ B (p65) (272 bp) sense 5'-TGGCGAGA GAAGCACAGATA-3' antisense 5'-TGTTGGTCTGGAT TCGCTG-3' and caspase-3 (sense 5'-GAGCACTGGAAT GTCATCTCGCTCTG-3' and antisense 3'-TACAGGAAG TCAGCCTCCACCGGTATC-5'. The genes were amplified against β -actin (287 bp) sense 5'-ATCCGTAAGACCTC TATGC-3' antisense 5'-AACGCAGCTCAGTAACAGTC-3'. The standard PCR products were generated by using positive control cDNA provided in the kit. The cycling conditions were as follows: 1 min at $94\text{ }^\circ\text{C}$, 1 min at $58\text{ }^\circ\text{C}$, and 1 min at $72\text{ }^\circ\text{C}$ for 40 cycles, followed by a 10-min extension at $72\text{ }^\circ\text{C}$. Amplified PCR products were electrophoresed on a 1.8 % agarose gel and stained with ethidium bromide and photographed under UV light.

Measurement of nitrite

HL-60 cells (5×10^5 cells) were pre-incubated at $37\text{ }^\circ\text{C}$ for 1 h in 0.5 ml of medium containing each **3** and **4** or the non-specific inhibitor of NOS N^G -monomethyl-L-arginine acetate (L-NMMA, Wako). After incubation for 12 h, nitrite levels in the conditioned medium were determined using Griess reagent (Mosmann, 1983).

Measurement of TNF- α

HL-60 cells (5×10^5 cells) were pre-incubated at $37\text{ }^\circ\text{C}$ for 1 h in 0.5 ml of medium containing each **3** and **4** or genistein. After 6 h incubation, TNF- α level in the conditioned medium were determined using a TNF- α enzyme-linked

immunosorbent assay (ELISA) kit (BioSource) according to the manufacturer's instructions.

Western blot analysis

HL-60 cells (2×10^6 cells) were incubated at 37 °C for 12 h in 2 ml of RPMI-containing 10 % FBS and the corresponding concentrations of each compounds **3** and **4**. After incubation, the cells were washed three times with PBS, dipped in 150 ml of ice-cold lysis buffer (20 mM HEPES, pH 7.4, 1 % Triton-X 100, 10 % glycerol, 1 M sodium fluoride, 2.5 mM *p*-nitrophenylene phosphate, 10 mg/ml of phenylmethylsulfonyl fluoride, 1 mM Na₃VO₄, 5 mg/ml of leupeptin, and 1 mM EDTA) for 15 min, and disrupted with a Sonic Disrupter (UR-20P, TOMY). The lysis buffer containing the disrupted cells was centrifuged at 13,000×*g* and 37 °C for 20 min. The supernatant fraction obtained was boiled for 5 min in 3× sample buffer (50 mM Tris, pH 7.4, 4 % SDS, 10 % glycerol, 4 % 2-mercaptoethanol, and 0.05 mg/ml of bromophenol blue) at a ratio of 2:1 (v/v), loaded on an acrylamide gel (8 or 10 %) and subjected to electrophoresis (150 min at 125 V). The antibody for iNOS, was purchased from Santa Cruz Biotechnology, and Western blotting was carried out as described previously (Ban *et al.*, 2002). The levels of each protein were quantified by scanning densitometry, and the individual band density value for each point was expressed as the relative density signal.

Statistical analysis

Values are expressed as the mean ± SD of three independent experiments. One-way analysis of variance (ANOVA) followed by Dunnett's test using Graph pad Instat Version 3.0 for Windows 95 (Graph Pad, San Diego, CA) were used to assess the statistical significance of the differences, with *p* values of less than 0.05 being considered statistically significant.

Acknowledgments Authors are thankful to Department of Biotechnology, Government of India for providing financial assistance for this study.

Conflict of interest Authors declare that there is no conflict of interest.

References

Abelson PH (1990) Medicine from plants. *Science* 247:513
 Ban HS, Lee SH, Kim YP, Yamaki K, Shin KH, Ohuchi K (2002) Inhibition of prostaglandin E2 production by taiwanin C isolated from the root of *Acanthopanax chiisanensis* and the mechanism of action. *Biochem Pharmacol* 64:1345–1354

Bunz F, Dutriaux A, Lengauer C, Waldman T, Zhou S, Brown JP, Sedivy JM, Kinzler KW, Vogelstein B (1998) Requirement for p53 and p21 to sustain G2 arrest after DNA damage. *Science* 282:1497–1501
 Chao JI, Kuo PC, Hsu TS (2004) Down-regulation of surviving in nitric oxide induced cell growth inhibition and apoptosis of the human lung carcinoma cells. *J Biol Chem* 279:20267–20276
 Crawford MJ, Krishnamoorthy RR, Rudick VL, Collier RJ, Kapin M, Aggarwal BB, Al-Ubaidi MR, Agarwal N (2001) Bcl-2 overexpression protects photooxidative stress-induced apoptosis of photoreceptor cells via NF-kappaB preservation. *Biochem Biophys Res Commun* 281:1304–1312
 Gallo O, Fini-Storchi I, Vergari WA, Masini E, Morbidelli L, Ziche M (1998) Role of nitric oxide in angiogenesis and tumour progression in head and neck cancer. *J Natl Cancer Inst* 90(8):587–596
 Ghisalberti EL (2000) *Lantana camara* L. (Verbenaceae). *Fitoterapia* 71:467–486
 Gschwind M, Huber G (1995) Apoptotic cell death induced by β-amyloid 1–42 peptide is cell type dependent. *J Neurochem* 65:292–300
 Haldar S, Basu A, Croce CM (1997) Bcl2 is the guardian of microtubule integrity. *Cancer Res* 57:229–233
 Hermeking H, Lengauer C, Polyak K, He T-C, Zhang L, Thiagalasingam S, Kinzler KW, Vogelstein B (1997) 14-3-3 sigma is a p53-regulated inhibitor of G2/M progression. *Mol Cell* 1:3–11
 Hong YS, Ham YA, Choi JH, Kim J (2000) Effects of allyl sulphur compounds and garlic extract on the expression of Bcl-2, Bax and p53 in non small cell lung cancer cell lines. *Exp Mol Med* 32(3):127–134
 Inada A, Nakanishi T, Tokuda H, Nishino H, Iwashina A, Sharma OP (1995) Inhibitory effects of Lantadenes and related triterpenoids on Epstein-Barr virus activation. *Planta Med* 61:558–559
 Inada A, Nakanishi T, Tokuda H, Nishino H, Iwashina A, Sharma OP (1997) Anti-tumor promoting activities of Lantadenes on mouse skin tumors and mouse hepatic tumors. *Planta Med* 63:272–274
 Kaur J, Sharma M, Sharma PD, Bansal MP (2008) Chemopreventive activity of Lantadenes on two-stage carcinogenesis model in Swiss albino mice: AP-1 (c-jun), NF κB (p65) and p53 expression by ELISA and immunohistochemical localization. *Mol Cell Biol* 314:1–8
 Kaur J, Sharma M, Sharma PD, Bansal MP (2010) Antitumor activity of Lantadenes in DMBA/TPA induced skin tumors in mice: expression of transcription factors. *Am J Biomed Sci* 2:79–90
 Lopez-Beltran A, MacLennan GT, de la Haba-Rodriguez J, Montironi R, Cheng L (2007) Research advances in apoptosis-mediated cancer therapy: a review. *Anal Quant Cytol Histol* 29:71–78
 Manchester KM, Heston WD, Donner DB (1993) Tumour necrosis factor induced cytotoxicity is accompanied by intracellular mitogenic signals in ME-180 human cervical carcinoma cells. *Biochem J* 290:185–190
 Mosmann T (1983) Rapid colorimetric assay for cellular growth and survival: application to proliferation and cytotoxicity assays. *J Immunol Methods* 65:55–63
 Sethi G, Shanmugam MK, Ramachandran L, Kumar AP (2012) Tergaonkar V (2012) multifaceted link between cancer and inflammation. *Biosci Rep* 32:1–15
 Sharma M, Sharma PD (2006) Optimization of lantadene isolation and preparation of 22β-hydroxy oleanonic acid. *Chem Nat Comp* 42:442–444
 Sharma OP, Dawra RK, Makkar HPS (1987) Isolation and partial purification of lantana (*Lantana camara* L.) toxins. *Toxicol Lett* 37:165–172
 Sharma OP, Sharma S, Dawra RK (1997) Reversed-phase high-performance liquid chromatographic separation and quantification of Lantadenes using isocratic systems. *J Chromatogr A* 786: 181–184

- Sharma M, Sharma PD, Bansal MP (2007a) Synthesis and antitumor activity of novel pentacyclic triterpenoid Lantadene D. *Lett Drug Des Discovery* 4:201–206
- Sharma M, Sharma PD, Bansal MP, Singh J (2007b) Lantadene A-induced apoptosis in human leukemia HL-60 cells. *Indian J Pharmacol* 39:140–144
- Sharma M, Sharma PD, Bansal MP, Singh J (2007c) Synthesis, cytotoxicity and antitumor activity of Lantadene A congener. *Chem Biodivers* 4:932–939
- Sharma M, Sharma PD, Bansal MP (2008) Lantadenes and their esters as potential antitumor agents. *J Nat Prod* 71:1222–1227
- Sharma M, Rakhi A, Dalal N, Sharma N (2011) Design, synthesis and evaluation of Lantadene A congener with hydroxyl functionality in ring A as an antitumour agent. *Nat Prod Res* 25:387–396
- Smith J, Williams GT, Kingston R, Jenkison EJ, Owen JJ (1989) Antibodies to CD3/T-cell receptor complex induce death by apoptosis in immature T cells in thymic cultures. *Nature (Lond)* 337:181–184
- Stepp JR, Moerman DE (2001) The importance of weeds in ethnopharmacology. *J Ethnopharmacol* 75:25–31
- Taylor WR, Stark GR (2001) Regulation of the G2/M transition by p53. *Oncogene* 20:1803–1815
- Yadav VR, Prasad S, Sung B, Kannappan R, Aggarwal BB (2010) Targeting inflammatory pathways by triterpenoids for prevention and treatment of cancer. *Toxins* 2:2428–2466
- Yonish-Rouach E, Resnitzky D, Lotem J, Sachs L, Kimchi A, Oren M (1991) Wild-type p53 induces apoptosis of myeloid leukaemic cells that is inhibited by interleukin-6. *Nature* 352:345–347